This is a repository copy of *Analysis of turbulence and surface growth models on the estimation of soot level in ethylene non-premixed flames*.

White Rose Research Online URL for this paper:
http://eprints.whiterose.ac.uk/127987/

Version: Accepted Version

Analysis of Turbulence and Surface Growth Models on the Estimation of Soot Level in Ethylene Non-Premixed Flames

Y. Yunardi[1], Edi Munawar[1], Wahyu Rinaldi[1], Asbar Razali[2], Elwina Iskandar[3] and M. Fairweather[4]

[1] Department of Chemical Engineering, Syiah Kuala University, Darussalam, Banda Aceh, Indonesia
[2] Department of Mechanical Engineering, Syiah Kuala University, Darussalam, Banda Aceh, Indonesia
[3] Department of Chemical Engineering, State Polytechnics of Lhokseumawe, North Aceh, Lhokseumawe, Indonesia
[4] School of Chemical and Process Engineering, University of Leeds, Leeds, United Kingdom

Soot prediction in a combustion system has become a subject of attention, as many factors influence its accuracy. An accurate temperature prediction will likely yield better soot predictions, since the inception, growth and destruction of the soot are affected by the temperature. This paper reported the study on the influences of turbulence closure and surface growth models on the prediction of soot levels in turbulent flames. The results demonstrated that a substantial distinction was observed in terms of temperature predictions derived using the k-ε and the Reynolds stress models, for the two ethylene flames studied here Amongst the four types of surface growth rate model investigated, the assumption of the soot surface growth rate proportional to the particle number density, but independent on the surface area of soot particles, f $(A_s) = \rho N_s$, yields in closest agreement with the radial data. Without any adjustment to the constants in the surface growth term, other approaches where the surface growth directly proportional to the surface area and square root of surface area, f $(A_s) = A_s$ and f $(A_s) = \sqrt{A_s}$, result in an under-prediction of soot volume fraction. These results suggest that predictions of soot volume fraction are sensitive to the modelling of surface growth.

Keywords: soot; conditional moment closure; combustion; surface growth; non-premixed; turbulent flame
.

Introduction

A characteristic of the combustion of fossil fuels in air is the formation and destruction of small solid carbonaceous soot particles within the combustion zone. The presence of such particles in a flame has a great impact on the nature and level of radiative heat transfer from the flame, and thus the temperature and structure of the reaction zones themselves. Therefore, accurate prediction of soot production in practical combustion systems is paramount for correctly estimating the radiation heat transfer from the reaction zones to cooler vicinities. In the case of non-sooting flames, for example, modelling is required to represent the turbulent flow fields and the interaction between turbulence and chemistry. Relating to the former, the standard k-ε and Reynolds stress turbulence models have been frequently used to obtain the flow condition for turbulent combustion systems [1,2]. With regard to sooting flames, the formation and destruction of soot a combustion system usually occurs in highly turbulent zones which involve the interaction of complex chemical and physical phenomena. Consequently, a precise prediction on soot production and destruction in such systems requires an integrated model enabling to couple turbulence, the interaction between turbulence and gas-phase chemistry, soot particle production and

removal, and radiation heat losses. The ability to apply such an integrated model, of demonstrated accuracy, to minimise soot production and emission in relation to safety and environmental considerations would represent a major step-forward in our ability to design and manage combustion processes.

In connection with turbulent combustion modelling, there has been a substantial progress in the last recent decades. A number of techniques have been proposed to challenge difficulty in modelling the chemical source term that appears in the species continuity equations. Among current proposed combustion models, the transported probability density function (PDF) approach [3] and the conditional moment closure (CMC) method [4] appear to offer the most promising features for future development. Both are capable of incorporating the detailed chemical mechanism into turbulent combustion computations, and thereby enable the prediction of minor chemical species and contaminants such as NOx and soot. The transported PDF method, which is generally based on Monte Carlo solution techniques, does, however, require substantial computer resources, whereas the deterministic CMC method requires a less restrictive approach to predicting combustion in practical geometries [4].

The challenge faced in the modelling of a turbulent sooty flame lies in the computation of soot production and destruction, due to the extreme complexity of chemistry of soot formation. Initial formation of soot and its later growth rely on tremendously complex chemical mechanism which could involve hundreds of species and several thousands of elementary chemical reactions. Difficulties and uncertainties in understanding sooting processes therefore impede progress in soot prediction. However, a number of models with different sophistication have been developed to describe the formation and oxidation of soot, and these have been applied in various combustion situations. These models use different physics and chemistry to describe the sooting process and can be categorized into three classes: purely empirical correlations, semi-empirical approach and detailed soot model.

At the initial phase of soot formation modelling development, predictions of soot levels in practical combustion systems entirely relied on empirical correlations. Empirical models do not require complex modelling since they were developed based on particular experimental data and are thus easy to implement and require little computer time [5, 6]. However, empirical models are not flexible and cannot be applied to different flows and combustion situations without adjustment. The next level of soot modelling, semi-empirical soot models attempt to explicitly incorporate various features of the physics and chemistry of the soot formation and destruction processes [7, 8]. In contrast to empirical models in which the soot formation phenomenon is treated globally, semi-empirical models start to couple the details of sooting sub-processes, such as soot particle inception, surface growth, coagulation and

agglomeration, and particle oxidation. Rate expressions are developed for each sub-processes represented by one- or two-step chemical reactions. Soot production is generally characterised by the total amount of the condensed phase, expressed as the soot volume fraction or soot mass fraction, and particle number density. Most models aim at solving transport equations for these two quantities, where the basic mechanisms of particle nucleation, surface growth, coagulation and oxidation enter the governing equations through the source terms [9,10]. The most sophisticated approach, detailed theoretical models employ detailed chemical kinetic and physical models to describe each sub-process that occurs in the gas phase, solid phase, and on the surface of soot particles. Detailed description of such sub-process necessitates to include numerous chemical species, up to benzene and higher aromatics. Consequently, this approach will require hundreds of chemical species and reactions [11]. Although such models are applicable over a wide range of combustion conditions, their application at present has been impaired by the excessive requirement for computer resources even for simple flames and the poor representation of soot inception chemistry, with some of the relevant reaction rates purely estimations [12]. Thus, for predictions of soot in practical engineering devices, it is often necessary to use simplified models to keep the computational cost at an acceptable level without losing a tolerable degree of accuracy.

This paper presented the results of a numerical simulation aimed at evaluating two different turbulence models, k-ε standard and Reynolds Stress Models, and soot surface growth modelling strategies for soot formation and destruction in ethylene turbulent non-premixed flames [14, 15]. A conditional moment closure (CMC) approach was

employed for modelling the combustion coupled with a semi-empirical soot model to represent the formation and destruction of soot in a flame [13]. Validations were performed by comparing the predictions by the model with the experimental data [14, 15].

Soot Surface Growth and CMC- Soot Modelling

Soot surface growth is primarily responsible for the mass accumulated in soot particles. It is commonly accepted that available surface area and the number of active sites on the surface are among the determining factors which influence the growth rate. However, the dependence of the soot surface growth rate on the surface area is still subject to debate in the literature, and many different approaches have been proposed. To investigate the influences of soot surface growth rates, four types of surface area functions are investigated in the present study.

The majority of works on semi-empirical soot modelling assume the growth rate to vary linearly with the available soot surface area [13, 16] and this constitutes the first function investigated in this study. Hence, the function of surface area is defined as f $(A_s)=A_s$. The next case assumes that the surface growth rate is proportional to the square root of the surface area, i.e. $f(A_s) = \sqrt{A_s}$. This assumption was introduced by Leung et al. [7] to consider changes in the amount of reactive surface area. The third case was based on a study [11] suggested that the growth rate is not only proportional to the surface area but also dependent on the surface chemistry. The soot surface reaction is assumed to take place through a sequential two-step process: H abstraction which creates an active site and C_2H_2 addition which propagates the surface growth. This H-abstraction-C_2H_2-addition reaction sequence is referred to as the HACA mechanism and is given by $C_s\text{-H+H} \leftrightarrow C_{s\bullet}\text{+H}_2$, $C_{s\bullet}\text{+H} \leftrightarrow C_s\text{-H}$ and the last one $C_{s\bullet}\text{+C}_2H_2 \leftrightarrow C_s\text{-H+H}$, where C_s-H represent an arm-chair site on the soot particle surface and $C_{s\bullet}$ the corresponding radical. The function of surface area can be expressed as $f(A_s) = \chi_s A_s$, where χ_s is the number density of surface radical and defined as Eq. 5. The last soot surface growth model which constitutes the simplest form of all is to assume that the mass growth reaction rate is proportional to the particle number density, but independent of the surface area, $f(A_s) = \rho N_s$ [13].

The detailed development of CMC transport equation can be found in Yunardi et al [8]. In addition to the CMC transport equation for species, the soot model employed in the present study [13] requires the solution of two additional CMC transport equations for the soot mass fraction, Y_s, and the soot particle number density, N_s, as presented in Eq. 1 and 2.

$$\frac{\partial Q_{Y_s}}{\partial x}\langle u|\eta\rangle^* = \left\langle \frac{\partial}{\partial x}\left(\rho D_\xi \frac{\partial \xi}{\partial x}\right)\Big|\eta\right\rangle + \left\langle w_{Y_s}|\eta\right\rangle$$
$$-0.4\frac{\left(Q_{Y_s} - Q_{Y_s}^+\right)}{\tau_\kappa(\eta)} \quad [1]$$

$$\frac{\partial Q_{N_s}}{\partial x}\langle u|\eta\rangle^* = \left\langle \frac{\partial}{\partial x}\left(\rho D_\xi \frac{\partial \xi}{\partial x}\right)\Big|\eta\right\rangle + \left\langle w_{N_s}|\eta\right\rangle$$
$$-0.4\frac{\left(Q_{N_s} - Q_{N_s}^+\right)}{\tau_\kappa(\eta)} \quad [2]$$

Eqs. 1 and 2 have been included with the effect of differential diffusion, which will not be further discussed here, since it has been examined in Yunardi et al [8]. The source term $\left\langle w_{Y_s}|\eta\right\rangle$ in Eq. 1 accounts for effects of soot nucleation, surface growth and oxidation, while the one in Eq. 2, $\left\langle w_{N_s}|\eta\right\rangle$, represents the influences of nucleation and agglomeration. In this study, acetylene and benzene compounds were chosen as the inceptive species responsible for soot nucleation. Nonetheless, acetylene was regarded as the only species which contributes to the increase in soot mass via surface growth. The soot nucleation proceeds via $C_2H_2 \leftrightarrow 2C_s + H_2$ and $C_6H_6 \leftrightarrow 6C_s + 3H_2$. It is assumed that surface growth carries on through acetylene reaction similar to the one in soot nucleation. Soot oxidation is assumed to proceed through $C_s + 0.5\,O_2 \to CO$ and $C_s + OH \to CO + H$. Now, the source terms for soot mass fraction and soot particle number density equations can be written as Eq.3 and Eq. 4.

$$\left\langle w_{Y_s}|\eta\right\rangle = 2k_1(Q_T)Q_{C_2H_2}M_s + 6k_2(Q_T)Q_{C_6H_6}M_s$$
$$+2k_3(Q_T)f(A_s)Q_{C_2H_2}M_s - k_4(Q_T)f(A_s)Q_{O_2}M_s \quad [3]$$
$$-k_5(Q_T)f(A_s)Q_{OH}M_s$$

$$\left\langle w_{N_s}|\eta\right\rangle = \left[2k_1(Q_T)Q_{C_2H_2} + 6k_2(Q_T)Q_{C_6H_6}M_s\right]\frac{N_A}{C_{min}}$$
$$-2C_a\left(\frac{6}{\pi}\frac{Q_{Y_s}}{\rho_\eta Q_{N_s}}\right)^{1/6}\left(\frac{6\kappa_B Q_T}{\rho_s}\right)^{1/2}\left(\rho_\eta Q_{N_s}\right)^2 \quad [4]$$

The surface area function, $f(A_s)$ in Eq. 3 will be investigated in accordance to (i) $f(A_s) = A_s$, (ii) $f(A_s) = \sqrt{A_s}$, (iii) $f(A_s) = A_s\chi_s$ and (iv) $f(A_s) = \rho N_s$. Values of reaction rate constants for nucleation, surface growth and oxidation that exist in Eqs. 3 and 4 are similar to those reported in Yunardi et al [17]. However, when $f(A_s) = A_s\chi_s$ the number density of surface radicals, χ_s is defined by Eq. 5 and values of constants that emerged in Eq. 5 are presented in Table 1. In the same equation, χ_{C3-H} represent the surface density of C_s-H sites, taken as 2.3×10^{19} site m^{-2}

[18]. The empirical factor, α, is adjustable and here is assigned as 1.0 [13]. M_s is the molar mass of soot, taken to be 12.011 kg kmol^{-1} and N_A is the Avogadro Number (6.022 x 10^{26}) kmol^{-1}. In the case of surface area function, f (A$_s$) = ρN_s. the reaction rate constants in Eqs. 3 and 4 are shown in Table 2.

$$\chi_s = \frac{\alpha k_{5.1,f} k_{5.3}[H]\chi_{C_{3-H}}}{k_{5.1,b}[H_2] + k_{5.2}[H] + k_{5.3}[C_2H_2]} \frac{M_s}{N_A} \qquad [5]$$

Table 1 Reaction rate constants for soot formation for f (A$_s$) = A$_s\chi_s$, in the form of the Arrhenius expression $k_j = AT^b \exp(-T_a/T)$ (units K, kmol, m, s) [18]

k_i	A	b	T_a
$k_{5,1,f}$	2.5 x 10^{11}	0	8,074
$k_{5,1,b}$	3.9 x 10^9	0	4,691
$k_{5,2}$	1.0 x 10^{11}	0	0
$k_{5,3}$	8.4 x 10^8	0.4	4,222

Table 2 Reaction rate constants for soot formation and oxidation for the case of f (A$_s$) = A$_s\chi_s$, in the form of the Arrhenius expression $k_j = AT^b \exp(-T_a/T)$ (units K, kmol, m, s) [13, 19]

k_i	A	b	T_a
k_1	1.0 x 10^4	0	21,000
k_2	0.75 x 10^5	0	21,000
k_3	0.1 x 10^{-13}	0	12,100
k_4	2.02 x 10^{-17}	0.5	19,680
k_5	2.77 x 10^{-17}	0.5	0

Experimental Conditions and Numerical Computation

The non-premixed ethylene flames considered in the present study were experimentally investigated Coppalle and Joyeux [14] and Young et al. [15], denoted from now on as flames CJ and YM. The burner of each flame consisted of a cylindrical nozzle with a diameter of 4.0 and 3.1 mm, respectively. Pure ethylene fuel issued into stagnant air of 1 atmosphere with bulk exit velocities of 29.5 and 24.5 m s^{-1}, which equal to exit Reynolds numbers of 11,800 and 8,600, respectively. The CJ fuel was preheated to 322 K, with the exception of flame YM, and in all flames a laser-extinction technique was used for the measurement of soot volume fraction along both the axial and radial directions. Temperature measurements were performed differently in the two flames, using thermocouples for the case of flame YM, and a two colour pyrometry technique for the case of flame CJ. Out of the two flames, flame YM presents axial and radial data on mean mixture fraction measured by microprobe sampling technique and spectrometric analysis.

The turbulent jet flames under consideration in this study are principally parabolic and axisymmetric in nature. The calculation of flow and mixing fields was therefore achieved by solutions of the axisymmetric forms of the partial differential equations which describe conservation of mass, momentum and the transport of mixture fraction and its variance. Two turbulence model closures, the Reynolds stress turbulence model and standard k-ε turbulence model were used. Closure of the mean density term was obtained by a prescribed β-PDF, with instantaneous values of density derived from adiabatic, equilibrium calculations based on the kinetic mechanism of Qin et al. [20]. Standard turbulence modelling constants appropriate to axisymmetric flows were employed to ensure the accurate prediction of the spreading rate of the jets.

Results of turbulent flow and mixing field calculations employing a reacting flow density were fed to the CMC model, where the set of species mass fractions, soot mass fraction, particle number density and enthalpy equations were solved in mixture fraction space. Solution of the CMC equations in real space was achieved using a fractional step method, implemented using the stiff ODE solver VODE, which applies a backward differentiation formula approach to solution of the non-linear equation set. Second-order differential sample space terms were determined using a central differencing approximation. The computational grids consisted of 68 radial nodes in mixture fraction space and 38 nodes in real space.

Results and Discussion
Effect of Turbulence Models on Temperature and Soot Predictions

Fig. 1 presents axial profiles of temperature and soot volume fraction, as well as radial profiles of soot volume fraction at two different downstream locations, in flame CJ [14]. The symbol denotes the experimental data, while solid and the dashed lines represent the simulations resulting from the application of the k-ε and the Reynolds stress models, respectively. The results show that the predicted temperature is in excellent agreement with data when flow field information from the k-ε is applied, with temperatures captured along the centreline of the flame, and with good agreement in terms of the magnitude and location of the peak temperature. These results are superior to those achieved using the transported PDF method [21, 22] and it should be noted that no adjustment was made to the enthalpy source term in the present work in order to obtain this level of agreement. Unfortunately, the experimental data lacks radial temperature profiles, so comparisons in this regard are not possible. With respect to results derived from its counterpart Reynolds stress model, temperature predictions are in line with the data up to approximately 500 mm along the centreline of the flame, but they then fall sharply and fail to follow the experimental trend.

Good agreement in the temperature predictions does not ensure accurate soot level results, as illustrated in the same figure, where axial and radial

soot concentrations are significantly under-predicted. This fact indicates that soot volume fraction is not only dependant on the temperature prediction but also on surface growth effect. Predictions of axial and radial distributions of soot volume fraction, and experimental values, are presented in the same Fig. 1. Here, the effect of differential diffusion of soot particles is not taken into account in determining the soot levels in the flames and also will not be discussed in this paper since it is out of the scope of the present investigation. For the purpose of investigating the effects of turbulence models, the surface growth rate for the prediction of soot level was assumed to be proportional to the surface area of soot particles, i.e. $f(A_s) = A_s$.
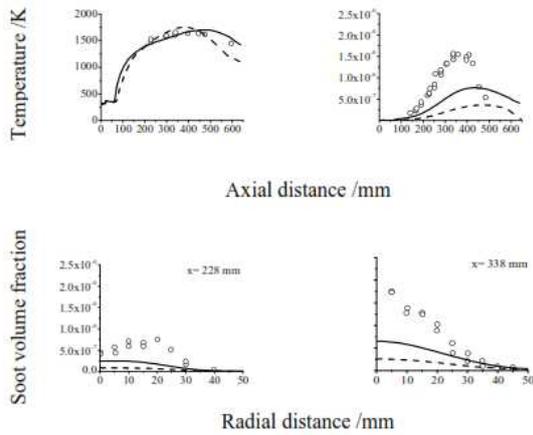

Fig. 1 Comparison of measured and predicted axial temperatures and soot volume fraction, and radial soot volume fractions at x = 228 and 338 mm for ethylene flame CJ (symbol - measured, — predicted k-ε, – – predicted Re stress).

Inspection of the axial profile shows that the agreement of predicted soot volume fraction and data is poor. The soot levels in the formation regions are significantly lower than the measurements, although predictions derived using the k-ε model are slightly better than those based on the Reynolds stress approach. Both turbulence models are, however, incapable of providing the CMC-based soot model with information that allows the accurate prediction of soot levels either qualitatively or quantitatively, in both the soot formation and oxidation regions, at least when the approximation that the surface growth rate is proportional to the local soot surface area is employed. The use of similar approaches by other authors also results in significantly low soot volume fractions, as observed by Ma et al. [23] in ethylene flames, and in methane flames [16]. Turning to the radial profiles given in the same figure, radial soot predictions are significantly underestimated in the mid-flame zone. However, there is a significant difference between results derived using the k-ε and the Reynolds stress models, in which soot predictions

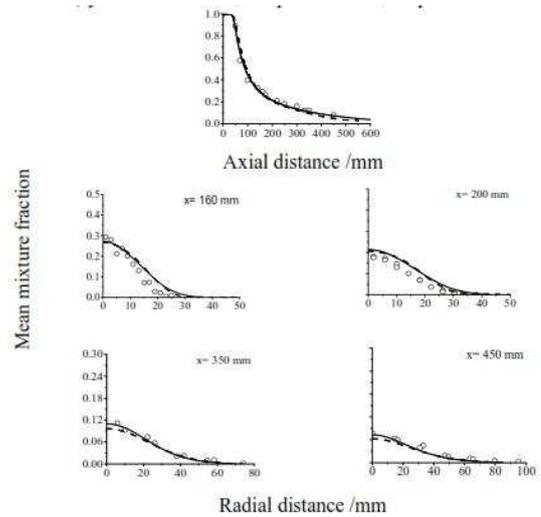are far better with the use of the k-ε turbulence model than those of Reynolds Stress Model.

Fig. 2 Comparison of measured and predicted axial and radial (at x = 160, 200, 350 and 450 mm) mean mixture fractions for ethylene flame YM (symbol - measured, — predicted k-ε, – – predicted Re stress).
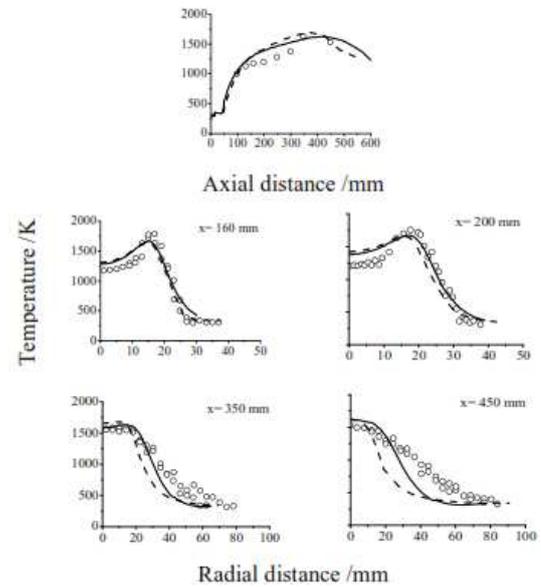

Fig. 3 Comparison of measured and predicted axial and radial (at x = 160, 200, 350 and 450 mm) temperatures for ethylene flame YM (symbol - measured, — predicted k-ε, – – predicted Re stress).

Flame YM [15] represents the second flame investigated in this study, and mixture fraction and temperature predictions on the centreline, in addition to radial values, are given in Figs. 2 and 3. It is clear that although both turbulence models capture centreline mean mixture fraction very well, the

predicted axial temperatures based on both turbulence models are less conforming. In the lower parts of the flame, particularly in the range between 150 and 350 mm above the nozzle, the temperature is over-predicted by up to 200 K. However, outside this range the temperature is in good agreement with data. A similar discrepancy is noted by Ma et al. [23] and Mauss et al. [24] when modelling this flame using a flamelet approach. The apparent form of the data in the range noted above could, however, be a consequence of using thermocouples to measure temperature, this being difficult to perform in the core of a sooting flame [24].
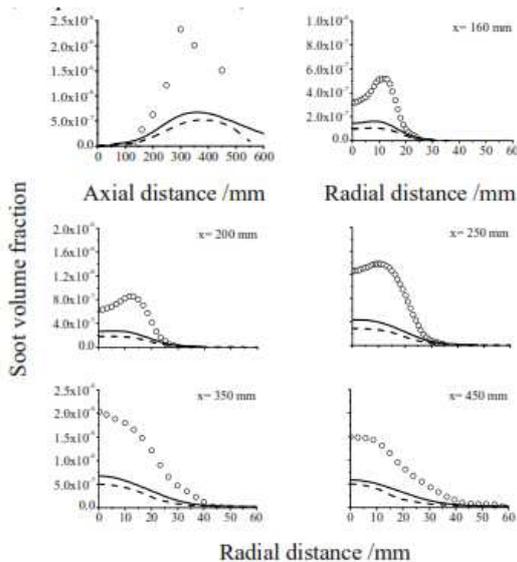

Fig. 4 Comparison of measured and predicted axial and radial (at x = 160, 200, 350 and 450 mm) soot volume fraction for ethylene flame YM (symbol - measured, — predicted k-ε, – – predicted Re stress).

Turning to the radial profiles in flame YM, both the k-ε and the Reynolds stress model predict mean mixture fraction fairly well, although in fuel-lean regions at x = 160 mm, and at all radii at x = 200 mm, over-predictions are clearly seen. Consistent with the axial temperature predictions, as presented in Fig. 3, temperatures at the core of the flame at x = 160 and 200 mm are over-predicted, although lean region temperatures are well represented. Further downstream, although predicted temperatures in fuel-rich regions at x= 350 and 450 mm are in reasonable agreement with data; poor agreement is obtained in the fuel-lean regions. The predicted radial temperature resulting from the Reynolds stress model provides even poorer agreement with data than for the k-e model with the progress of the axial height in the flame. Except for the profile at x = 160 mm, where results generally conform with data, previous studies [23, 24] do not present radial temperature predictions at other axial locations, and hence no comparison can be made with the present results. Inspection of soot

volume fractions in Fig. 4, again it shows that soot volume fractions are significantly under-predicted by the CMC – soot model in both the axial and radial profiles. However, soot predictions derived using flow-field resulted from the use of k-ε turbulence model are slightly better than that of Reynolds stress model.

It has been demonstrated that there is a significant difference in terms of temperature predictions derived using the k-ε and the Reynolds stress models, for the two ethylene flames studied here, although this is not the case for the soot volume fraction calculations. In most cases, predictions in terms of mixture fraction, temperature and soot volume fraction are in better agreement with measured values when the flow field is calculated with the k-ε turbulence closure, instead of the Reynolds stress model. These results implied that flow-field information obtained from more complex turbulence models and implemented in CMC-soot computation do not always give better predictions than those of simpler turbulence models.

Effect of Surface Growth Models on Soot Level Predictions

Figs. 5 and 6 illustrate the results of using four different types of surface area function on soot level predictions in the two ethylene flames. The solid line describes the function of surface area equivalent to the surface area of the soot particles, the dashed line represents the surface growth proportional to the square root of surface area, while the dotted line refers to a function of surface area which is not only proportional to the surface area but also the surface chemistry, from now on referred to as the HACA mechanism. The final dashed-dot-dashed line depicted the surface area function equivalent to the particle number density.

Inspection of Fig. 5, in both axial and radial profiles, distinct differences amongst the surface area model types are clearly seen. Amongst the four types of model, assuming the soot surface growth rate to be proportional to the particle number density, but independent of the surface area of the soot particles, f (A_s) =ρN_s yields in closest agreement with the axial and radial data of CJ flame. A similar level of agreement with the application of this type of surface area model can also been seen in the radial profiles of flames YM in Fig. 6. Although predicted results are encouraging, the model is clearly incapable of producing accurate soot oxidation results in either the axial or radial direction. Predictions may be improved by performing adjustments to the activation temperature used in this model. Although the influence of such adjustments is most appropriately assessed by comparison with laminar flame data, rather than in the turbulent flames which are the focus of the present investigation. Lindstedt [13] argued that adjustments to the proportionality of the surface area function to the particle number density can

improve predicted results, although it is important to note that improved agreement was only achieved by adjusting the Arrhenius constant in the surface growth rate term, thereby reducing the generality of the model.
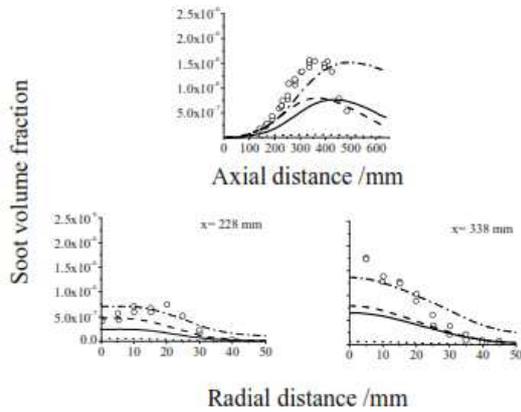

Fig. 5 Comparison of measured and predicted axial and radial (at x = 228 and 338 mm) soot volume fractions for ethylene flame CJ (symbol - measured, — predicted f (A_s) = A_s, --- predicted f (A_s) = $\sqrt{A_s}$, ···· predicted f (A_s) = $A_s\chi_s$, —·— predicted f (A_s) =ρN_s)
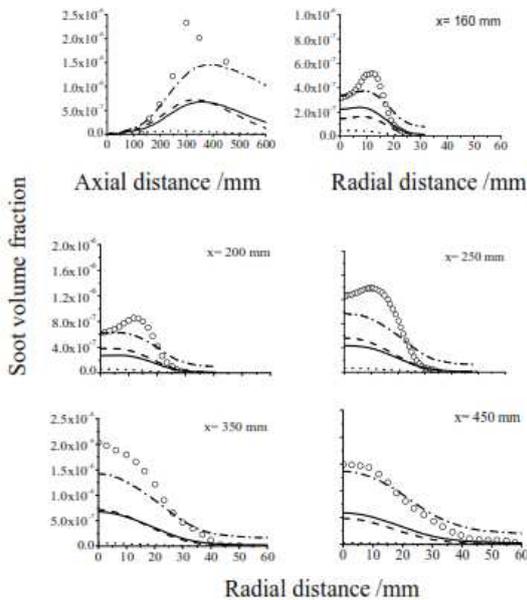

Fig. 6 Comparison of measured and predicted axial and radial (at 160, 200,250, 350 and 450 mm) soot volume fractions for ethylene flame YM (symbol - measured, — predicted f(A_s) = A_s, --- predicted f(A_s) = $\sqrt{A_s}$, ···· predicted f(A_s) = $A_s\chi_s$, —·— predicted f(A_s) =ρN_s)

In view of the complexity of the HACA surface growth model [11], it is surprising that this approach produces such a low soot volume fraction prediction in all ethylene flames under investigation. Frenklach and Wang [11] validated the model against several premixed flames, and obtained reasonable agreement with experimental data. However, Lindstedt [13] could not produce acceptable predictions with the use of the HACA growth model when applied to modelling soot formation in counter-flow ethylene flames. The author [13] argued that the premixed flames investigated by Frenklach and Wang [11] concerned very small soot particles of less than 5 nm, producing low soot volume fractions. Contrastingly, the present study involves significantly larger particles of more than 50 nm, and consequently higher soot volume fraction.

Ma et al. [23] also investigated the effect of various surface growth models and found that the assumption of surface growth proportional to the square root of the surface area can improve soot volume fraction predictions. Results in the present study, however, show that whilst such an approach does result in a minor improvement in soot volume fraction prediction, it does not significantly outperform the commonly used model which assumes the surface growth proportional to the surface area. Without any adjustment to the constants in the surface growth term, both approaches where f (A_s) = A_s, and f(A_s) = $\sqrt{A_s}$ result in an under-prediction of soot volume fraction,

Conclusions

A first-order CMC-based soot model has been applied to the calculation of soot levels in two turbulent non-premixed ethylene flames, with the aim at investigating the influences of turbulence closure and surface growth rate models. From the results and discussion, the following conclusions can be drawn:

1. A lack of experimental data prevents a detailed analysis of flow field predictions obtained using the k-ε and Reynolds stress turbulence models. However, the results obtained demonstrate that predictions derived from the k-ε closure are superior to those derived using the Reynolds stress model. There is clearly a requirement for more detailed flow field measurements of sooting ethylene flames.

2. Predictions of soot volume fraction are sensitive to the modelling of surface growth. A complex model of this process which includes surface chemistry [11], did not produce an acceptable level of agreement with data in comparison to simpler models. Amongst the four surface area functions studied, the assumption of soot surface growth rate to be proportional to the particle number density, but independent of the surface area of the soot particles, f (A_s) =ρN_s yields in closest agreement with the experimental data, although discrepancy is evident in the oxidation region.

3. In general, predictions of mean mixture fraction, temperature and soot volume fraction in the three flames studied show good to excellent qualitative and quantitative agreement with data, and compare favourably with the results of earlier investigations of these flames that employed flamelet

and transported PDF approaches. With respect to axial temperature predictions, an over-prediction occurs within the lower part of flame YM. However, an excellent representation of temperatures is obtained along the core of flame CJ, indicating that the assumptions of the radiation model employed are satisfactory. The latter is also confirmed by the accuracy of peak radial temperature predictions obtained in all two flames.

Acknowledgment

References

[1] Fairweather, M. and Woolley, R.M. First-order conditional moment closure modelling of turbulent, non-premixed methane flames. Combust. Flame, Vol. 138 (2004): 3-19.

[2] Fairweather, M., Woolley, R.M. and Yunardi, Analysis of kinetic mechanism performance in conditional moment closure modelling of turbulent, non-premixed methane flames. Combust. Theor. Model. Vol. 10 (2006): 413-438.

[2] Pope, S.B., PDF methods for turbulent reactive flows. Prog. Energy Combust. Sci., Vol. 11 (1985): 119-192.

[4] Klimenko, A.Y. and Bilger, R.W., Conditional moment closure for turbulent combustion. Prog. Energy Combust. Sci., Vol 25 (1999): 595-687.

[5] Calcote H. F. and D. M. Manos. Effect of molecular structure on incipient soot formation. Combust. Flame, Vol. 49 (1983): 289-304.

[6] Micklow GJ, Gong W. A multistage combustion model and soot formation model for direct-injection diesel engines. Proc Inst Mech Eng Part D: J Automobile Eng., Vol. 216 (2002):495–504.

[7] Leung, K.M., Lindstedt, R.P., Jones, W.P., A simplified reaction-mechanism for soot formation in non-premixed flames. Combust. Flame, Vol., 87 (1991): 289-305.

[8] Moss, J.B., Stewart, C.D. and Syed, K.J. Flow field modeling of soot formation at elevated pressure. Proc. Combust. Inst., Vol. 22 (1988): 413-423.

[9] Yunardi, Woolley,R.M. and Fairweather, M. Conditional moment closure prediction of soot formation in turbulent, non-premixed ethylene flames. Combust. Flame, Vol.152 (2008): 360–376.

[10] Mazzei, L, Puggelli, S., Bertini, D., Pampaloni D., and Andreini, A., Modelling soot production and thermal radiation for turbulent diffusion flames Modelling soot production and thermal radiation for turbulent diffusion flames. Energy Procedia, Vol. 126 (2017): 826-833

[11] Frenklach, M. and Wang, H., (1994), Detailed mechanism and modeling of soot particle formation. In H. Bockhorn (Ed.), Soot formation in combustion (pp. 165–190), Springer, Berlin.

[12] Wen, J.Z., Thomson, M., Park, S., Rogak, S. and Lightstone, M., Study of soot growth in a plug flow reactor using a moving sectional model. Proc. Combust. Inst., Vol. 30 (2005): 1477-1484.

[13] Lindstedt, R.P. (1994), Simplified soot nucleation and surface growth steps for nonpremixed flames. In H. Bockhorn (Ed.), Soot formation in combustion (pp. 417-441), Springer-Verlag, Berlin.

[14] Coppalle, A and Joyeux, D, Temperature and soot volume fraction in turbulent diffusion flames: measurements of mean and fluctuating values. Combust.Flame, Vol.96 (1994): 275-285.

[15] Young, K.J., Stewart, C.D., Syed, K.J, and Moss, J.B., Soot formation in confined flames fuelled by pre-vaporized kerosene and ethylene. Proceeding of the Tenth ISABE Meeting, AIAA (1991): 239-248.

[16] Kronenburg, A., Bilger R. W., and Kent, J. H. Modeling soot formation in turbulent methane–air jet diffusion flames. Combust. Flame, Vol. 121 (2000): 24-40.

[17] Yunardi, Y., Darmadi, D., Hisbullah, H H., Fairweather, M., Investigation of detailed kinetic scheme performance on modelling of turbulent non-premixed sooting flames, J. Therm. Sci, Vol.20 (2011): 548-555

[18] Xu F., Lin K.C. and Faeth G.M., Soot formation in laminar premixed methane/oxygen flames at atmospheric pressure. Combust. Flame, Vol. 115 (1998): 195-209.

[19] Louloudi, S.A., (2003), Transported probability density function modelling of turbulent jet flames. PhD thesis, Imperial College London.

[20] Qin, Z., Lissianski, V.V.,Yang, H., Gardiner, W. C., Davis, S. G. and Wang, H., Combustion chemistry of propane: A case study of detailed reaction mechanism optimization. Proc. Combust. Inst., Vol. 28 (2000): 1663-1669.

[21] Lindstedt, R.P. and Louloudi, S.A., Joint-scalar transported PDF modeling of soot formation and oxidation. Proc. Combust. Inst., Vol. 30 (2005): 775-783.

[22] Zamuner, B. and Dupoirieux, F., Numerical simulation of soot formation in a turbulent flame with a Monte Carlo PDF approach and detailed chemistry. Combust. Sci. Technol., Vol. 158 (2000): 407-438.

[23] Ma, G., Wen, J.Z., Lightstone, M.F. and Thomson, M.J., Optimization of soot modelling in turbulent non-premixed ethylene/air jet flames. Combust. Sci. Technol., Vol. 177 (2005): 1-36.

[24] Mauss, F., Netzell, K. and Lehtiniemi, H., Aspects of modelling soot formation in turbulent diffusion flames. Combust. Sci. Technol., Vol. 178 (2006): 1871-1855.